RESEARCH ARTICLE

miR-29b inhibits non-small cell lung cancer progression by targeting STRN4

Yuping Xie[1] · Fen Zhao[1] · Ping Zhang[1] · Ping Duan[1] · Yangmei Shen[2]

Abstract

Non-small cell lung cancer (NSCLC) is a malignant tumor with a high fatality, low overall cure, and survival rates worldwide. When only palliative therapy is available, the disease leads to malignant proliferation. Previous studies showed miR-29b serves as an NSCLC suppressor by inhibiting cells proliferation, migration, and invasion. However, the mechanism underlying NSCLC progression remains elusive. In this study, we identified Striatin 4 (STRN4), a target of miR-29b, which serves as a pro-oncogenic protein by promoting cells proliferation, migration, and invasion in NSCLC. Besides, the STRN4 was highly expressed in NSCLC and negatively regulated by miR-29b. Down-regulation of STRN4 inhibits NSCLC cells proliferation, migration, invasion, and promotes apoptosis in vitro, whereas overexpression-induced enhanced cell migration and invasion could be reverred by miR-29b. Notably, overexpression of miR-29b and down-regulation of STRN4 by shRNA suppressed cellular proliferation and delayed tumor progression in vivo. Together, these findings identify a miR-29b/STRN4 regulatory pathway in NSCLC progression, which may provide a new sight for the treatment of NSCLC.

Keywords miR-29b · STRN4 · Non-small cell lung cancer · Progression · Overexpression

Introduction

Lung cancer is the leading cause of cancer death in the world, with an estimated 1.6 million deaths each year [1]. It has been estimated that about 85% of patients with lung cancer are NSCLC [2]. However, the overall survival and cure rates of NSCLC remain low. Therefore, further research into the disease biology and mechanisms of malignant proliferation is required to increase our understanding of NSCLC and improve the survival rate.

Numerous studies have revealed microRNAs (miRNAs), small noncoding RNAs that have the capacity to regulate gene expression, are implicated in cancer initiation and progression [3, 4]. Aberrant patterns of miRNA expression have been reported in multiple cancers, and they have been demonstrated to act as key factors in cancer at all stages, ranging from initiation to metastasis [5]. The miR-29 family (miR-29s) contains miR-29a, miR-29b, and miR-29c in humans. The structure, function, and regulation of the miR-29s are highly similar in humans and rodents [6]. The Kirsten ras oncogene (KRAS) mutation is one of the most common mutations in lung cancer [7], and the miR-29b can be driven by KRAS through the RAF–MEK–ERK pathway [8]. In addition, miR-29b functions as a tumor suppressor in breast cancer cells and inhibits the invasion and angiogenesis of cervical cancer by targeting STAT3 [9–11]. Previous studies have revealed a down-regulation of miR-29s, including the miR-29b, in NSCLC [12–14]. Further studies showed that loss of tumor-suppressive miR-29s promoted cancer cell invasion in lung squamous cell carcinoma [15], while up-regulation of miR-29 attenuated NSCLC metastasis [12]. The molecular targets of miR-29b in NSCLC have been reported. Recently, Chen et al. demonstrated that the miR-29 family could directly target SET domain bifurcated-1 (SETDB1) in NSCLC [13]. And Wang et al. reported that miR-29b suppressed NSCLC metastasis in vitro and in vivo by directly targeting 3′-UTR of Phosphatase and Tensin homolog deleted on chromosome Ten (PTEN) and Matrix Metalloprotein 2 (MMP2) mRNAs and down-regulated MMP2 protein expression [12]. However, it is not clear

✉ Yangmei Shen
zhili0309@163.com

[1] Department of Oncology, Chengdu City First People's Hospital, Chengdu 610041, People's Republic of China

[2] Department of Pathology, West China Second University Hospital, Sichuan University, Chengdu 610041, People's Republic of China

whether other downstream targets of miR-29b are involved in NSCLC progression.

Emerging evidence shows STRN4, a member of the striatin family interacts with a diverse set of proteins (e.g., calmodulin and caveolin), is widely expressed in the nervous system as well as in other tissues and cell lines [16–19]. Previous studies suggest that STRN4 regulates dendritic growth and rodent's behaviors [20–22]. Of note, STRN4 plays a pivotal role in pancreatic cancer malignancy by promoting the proliferation, migration, invasion, and anchorage-independent growth of cancer cells [23]. Accumulating evidence has revealed that up-regulated STRN4 is associated with germinal center kinases that exert tumor-promoting or tumor-suppressing activity [24–26]. In addition, Fan et al. reported that miR-873 inhibited colorectal cancer metastasis by directly binding to the 3′UTRs of ELK1 and STRN4 [27]. However, there is a lack of information about whether STRN4 involves in the progression of NSCLC.

In this study, we performed bioinformatics analysis to explore the downstream targets of miR-29b, and found that STRN4 may be a novel candidate target of miR-29b. Further luciferase reporter assays revealed that miR-29b interacted with STRN4 by directly targeting its 3′UTRs. And the STRN4 was highly expressed in NSCLC. In addition, miR-29b reversed STRN4-induced enhancement of NSCLC cell apoptosis, migration, and invasion. These results provide new sights into the molecular mechanism and therapy of NSCLC.

Materials and methods

Patient samples

We collected 40 NSCLC tissue samples from the years 2015 to 2018, after surgical resection at the West China Second University Hospital (Sichuan, China). Patients who had any anticancer therapy before tissue sample collection were excluded. The tumor stage was characterized using guidelines from the 2010 American Joint Committee on Cancer and the International Union against Cancer Tumor-Node-Metastasis (TNM) classification system, and the tumor differentiation was graded according to the Edmondson and Steiner grading system. This study was approved by the Ethics Committee of West China Second University Hospital, and all patients provided written informed consent.

Cell culture and chemicals

The subtypes of the non-small cell lung cancer cell lines, namely, A549, NCI-H460, PC9, and NCI-H441, were purchased from the Cell Bank of the Chinese Academy of Sciences (Shanghai, China). The cells were cultured in Dulbecco's Modified Eagle's Medium (DMEM, Gibco, USA), supplemented with 10% heat-inactivated fetal bovine serum (FBS), 2 mM L-glutamine, and antibiotics (0.1 mg mL^{-1} streptomycin and 100 U mL^{-1} penicillin). All cells were cultured in a 37 °C incubator with 5% CO_2. Anti-STRN4 (ab177155), Anti-p21 (ab109199), Anti-cyclinD1 (ab16663), Anti-Bax (ab32503), Anti-E-cadherin (ab1416), Anti-MMP-9 (ab73734), and GAPDH (ab181602) antibodies were purchased from Abcam (Cambridge, MA, USA). The miR-29b-3p mimics (5′-UAGCACCAUUUGAAAUCAGUGUU-3′, 5′-UAGCACCAUUUGAAAUCAGUGUU-3′) and inhibitors (5′-AACACUGAUUUCAAAUGGUGCUA-3′) were purchased from RiboBio Co., Ltd. (Guangzhou, China). The shRNA STRN4-1 (CCGGGCTAGATGTGGAACCTATACCTCGAGGTATAGGTTCCACATCTAGCTTTTTG), and shRNA STRN4-2 (CCGGGCCTCTGTCTGTTTGCCATGGCTCGAGCCATGGCAAACAGACAGAGGCTTTTTG) specific for STRN4.

Generation of stable cell lines

A549 cells that expressed shRNA-STRN4 or miR-29b-3p were established by retroviral infection and selected by puromycin. The shRNA STRN4-1, pre-miR-29b-3p, and negative control (NC) that packaged in lentivirus were bought from Hefei Zhien Biotech. Co. (Hefei, China). The A549 cells were seeded into 6-well plates, and the lentivirus with the best multiplicity of infection (MOI) was added for 24 h, then puromycin (5 µg/mL, Sigma-Aldrich) was added to the culture for a specific selection of the infected cells.

Proliferation assay

The viability of cells was analyzed by the standard MTT [3-(4, 5-dimethylthiazol-2-yl)-2, 5-diphenyltetrazolium bromide] reagent (Roche, Basel, Switzerland) assay. Cells were seeded into 96-well plates (5×10^3 cells/well) at 37 °C. The cell culture (100 µl) and MTT solution (10 µl/well) were mixed well and added into the wells, which were incubated with 5% CO_2 for 4 h at 37 °C. A microplate reader (Bio-Rad, USA) was used to measure the absorbance at 490 nm.

Flow cytometry

For the cell-cycle analysis, cells were collected and centrifuged in a centrifuge at 600g for 10 min. The pellet was fixed with cold 70% ethanol for 2 h at 4 °C and then centrifuged at 3000g for 5 min, followed by resuspension in 100 µl PBS and incubation with 5 µl RNAse (20 µg/ml) for 30 min at 37 °C. Then, the cells were stained with propidium iodide (50 µg/ml) for 30 min and counted using an Accuri™ C6 flow cytometer (BD Biosciences). The results were analyzed using ModFit S software.

For the apoptosis analysis, cells were collected and resuspensed in 500 μl binding buffer. Subsequently, they were stained with 5 μl (250 μg/ml, final concentration) Annexin V mixed with 5 μl propidium iodide (1 μg/ml, BD Biosciences). Stained cells were quantified by an Accuri™ C6 flow cytometer, and the data were displayed on a graph by FlowJo software version 10 (FlowJo LLC, USA). All experiments were conducted in triplicates.

Migration and invasion assay by Transwell assay

The Transwell assay was used to estimate the migration and invasion ability of cells. Cells were detached by digestion with 0.25% trypsin, then re-suspension using DMEM without serum to 1×10^5 cells/ml. Transwell membranes with 8-mm-pore size (Corning Inc. USA) were placed into the wells of the 24-well plates containing 600 μl DMEM with 10% FBS. After the membranes were seeded with 200 μl of cultured cells in culture medium and incubated for 24 h in a 5% CO_2 incubator, the cells were fixed on the Transwell membranes with 4% polyformaldehyde and stained with 0.5% crystal violet solution for 5 min and rinsed again with water for 5 min. Images were captured by a microscope (Leica, DM2500, Germany). For the invasion assay, the cells were seeded on the pre-coated Matrigel (BD Biosciences) of the polyethylene terephthalate membranes.

Wound healing assay

The 5×10^5 cells were seeded into each well of plates and allowed to grow to a confluent monolayer in a 37 °C incubator before wounding the monolayer by scratching the surface with a pipette tip. Next, the cells were washed three times, replacement with fresh medium to continue culture for 24 h. The images of cell migration were captured with a microscope (Leica, DM2500, Germany).

Immunohistochemical staining

The tissue specimens were fixed with formalin and embedded in paraffin blocks, and then sliced into 6-μm thick sections. After antigen retrieval and blocking, the sections were incubated with STRN4 antibody at 4 °C overnight. After staining, the images were visualized and captured with a microscope (Zeiss, Germany).

Real-time polymerase chain reaction (RT-PCR)

Trizol reagent (Invitrogen) was used to extract total RNA from tissues or cells, according to instructions from the manufacturer. The purity and concentration of the isolated total RNA were measured using a UV spectrophotometry. Then, the cDNA was synthesized using a qRT-PCR kit (TransGen) and amplified in a reaction mixture containing 10 μl of master mix SYBR Green, 1 μl of each primer of STRN4 (forward: GATCTCACCGTCACCAACGA; reverse: GGAACGAATGCCGTCGTAGT), 1 μl cDNA template, and 8 μl ddH$_2$O. The expression levels of STRN4 were normalized to those of the housekeeping gene, glyceraldehyde 3-phosphate dehydrogenase (GAPDH, forward: AATCCC ATCACCATCTTCCA; reverse: GGCGGAGATGATGAC CCTT). The relative gene expression was calculated with the LightCycle Application (LC96, USA).

Western blotting

Protein lysates from cells were prepared by using a lysis buffer. The proteins were purified after centrifugation. The protein sample was separated using gel electrophoresis, and transferred to the membrane using previously a described method [28]. After blocking with 5% non-fat milk on a shaking bed and then incubated with the primary antibodies against STRN4 (1:1000) and GAPDH (1:1000) and subsequently incubated with relevant anti-rabbit IgG-HRP (1:5000, CST) and goat anti-mouse IgG-HRP (1:5000, CST) secondary antibodies. Finally, the visualization of protein bands was accomplished with a gel imaging system (Fusion Solo, France). The quantification of the bands' signals was performed using by ImageJ software.

Bioinformatics

The gene *STRN4* was predicted to be targeted by miR-29b using TargetScan (www.targetscan.org). Using three independent prediction programs (miRecords, mirecords.biolead. org; miRGator, genome.ewha.ac.kr/miRGator/miRGator. html; miRGen, www.diana.pcbi.upenn.edu/miRGen.html) to perform comparative analyses to confirm the accuracy of the prediction.

Luciferase reporter assays

Luciferase reporter assays were performed as previously described previously [29]. Briefly, 293T cells were seeded into 24-well plates at 70–80% confluency, 1 day prior to transfection. miR-29b-3p mimics and NC mimics were co-transfected with the reporter vector STRN4 wild-type (3′UTR-WT) or STRN4 mutated-type (3′UTR-MUT) into the 293T cells, using Lipofectamine 2000 (Invitrogen) transfection reagent and incubated for 6 h according to instructions from the manufacturer. Forty-eight hours after transfection, luciferase activity was measured using the Dual-Luciferase® Reporter Assay System (Promega Corporation, Fitchburg, WI, USA).

EdU staining

Cells were seeded into 24-well plates and incubated for 2 h with a preheated EdU working solution (10 M) at 37 °C. The cells were washed 3 times and a permeable solution was added to 24-well plates for incubating 10–15 min. After washing 3 times, 200 µl Click reaction mixture was used to incubate 30 min at room temperature in the dark. Following washing 3 times, the images were observed and captured with a microscope.

Animal experiments

Animal experiments were conducted in accordance with the regulations of Sichuan University. A total of 2×10^6 cell(1×10^7 cell/mL, 200 µl) control, miR-29b-3p overexpressing, and shRNA-STRN4 lung cancer cells were injected s.c. into both sides of the femoral area of six nude mice. The mice were killed 4 weeks after tumor inoculation, and the tumors were extracted to determine their volumes and weights. A caliper was used to measure tumor diameter, and tumor volume was calculated using the following formula: $\pi/6 \times (\text{largest diameter})^3$.

Statistics

All statistical analyses and graphing were performed using SPSS software (version 22; SPSS Inc., Chicago, IL, USA) and the GraphPad Prism 7 (Graph Pad Software, Inc., USA). All data were expressed as mean $\pm$ standard deviation. To test the significance of the data, Student's t test, ANOVA analysis, and Spearman's rank correlation were used. A p value of < 0.05 represented statistical significance.

Results

miR-29b negatively regulate STRN4 expression by directly targeting 3′UTR region

Previous studies reported miR-29b suppressed NSCLC metastasis in vitro and in vivo [12]. In an effort to find the downstream target of miR-29b in NSCLC, we first performed a bioinformatic analysis using TargetScan and found PTEN, MMP2, and STRN4 were potential target molecules of miR-29b. Unlike PTEN and MMP2 that have been demonstrated by Wang et al. [12], STRN4 is a novel target of miR-29b that has never been reported. Given the important role of STRN4 in cancer cell proliferation, migration, and invasion [23, 27]. The luciferase reporter assays were employed to further determine whether miR-29b can directly target the 3′UTR region of STRN4. After cloning the target sequence (3′UTR-WT) or MUT sequence (3′UTR-MUT)

into a luciferase reporter vector, and transfecting 293T cells with the WT or MUT 3′UTR vector and miR-29b-3p mimic or control mimic (Fig. 1a). We observed an obvious decrease of the luciferase activity in WT vectors after co-transfecting with miR-29b-3p mimic, and a mutation in the putative binding site within the STRN4 3′UTR region abrogated the suppressive effect of miR-29b-3p mimic (Fig. 1b). To further examine the interplay between miR-29b and STRN4 in the NSCLC, four subtypes of the NSCLC cell lines, namely A549, NCI-H460, PC9, and NCI-H441, were screened for their STRN4 mRNA and protein expressions. Compared with NCI-H460 and NCI-H441 cell lines, the expression of STRN4 mRNA and protein in A549 and PC9, especially in PC9 cells, were higher (Fig. 1c, d). Then both the A549 and PC9 cells were transfected by the WT/MUT 3′UTR vector and miR-29b-3p/control mimic, we found that the miR-29b was able to repress STRN4 expression at both the mRNA and protein levels in A549 and PC9 cells (Fig. 1e, f). Together, these results indicate miR-29b negatively regulate STRN4 expression by directly targeting its 3′UTR region in NSCLC cells.

Upregulated STRN4 in NSCLC tissues and cell lines

To investigate the function of STRN4 in NSCLC, we next examined the expression levels of STRN4 in NSCLC tissues (tumor, $n = 40$) and corresponding paracancerous tissues (normal, $n = 40$) by immunofluorescence. Immunofluorescence stains showed STRN4 located both in the cytoplasm and cytomembrane, the number and fluorescence intensity of STRN4 positive cells significantly increased in NSCLC tissues compared with those of the normal tissues (Fig. 2a). Using RT-PCR and western blotting approaches, we found higher STRN4 mRNA and protein expressions in NSCLC tissues than the corresponding paracancerous tissues (Fig. 2b, c). Together, these results suggest increased expression of STRN4 in NSCLC. Besides, the STRN4 expression in NSCLC cells was also analyzed. Consistent with the results obtained from the NSCLC tissue, the expression of STRN4 mRNA and protein in A549 and PC9 cell lines is much higher than that of the normal lung epithelial cell lines, namely, HFL-1 and HBEC (Fig. 2d, e). Given the higher expressions of STRN4 in A549 and PC9 cells, we next focused on its biological role in cell proliferation, migration, invasion, and apoptosis in A549 and PC9 cell lines.

STRN4 knockdown inhibits NSCLC cells proliferation, migration, and invasion and promotes apoptosis in vitro

We first used two different kinds of shRNA-STRN4 (shRNA STRN4-1 and shRNA STRN4-2) to knock down STRN4
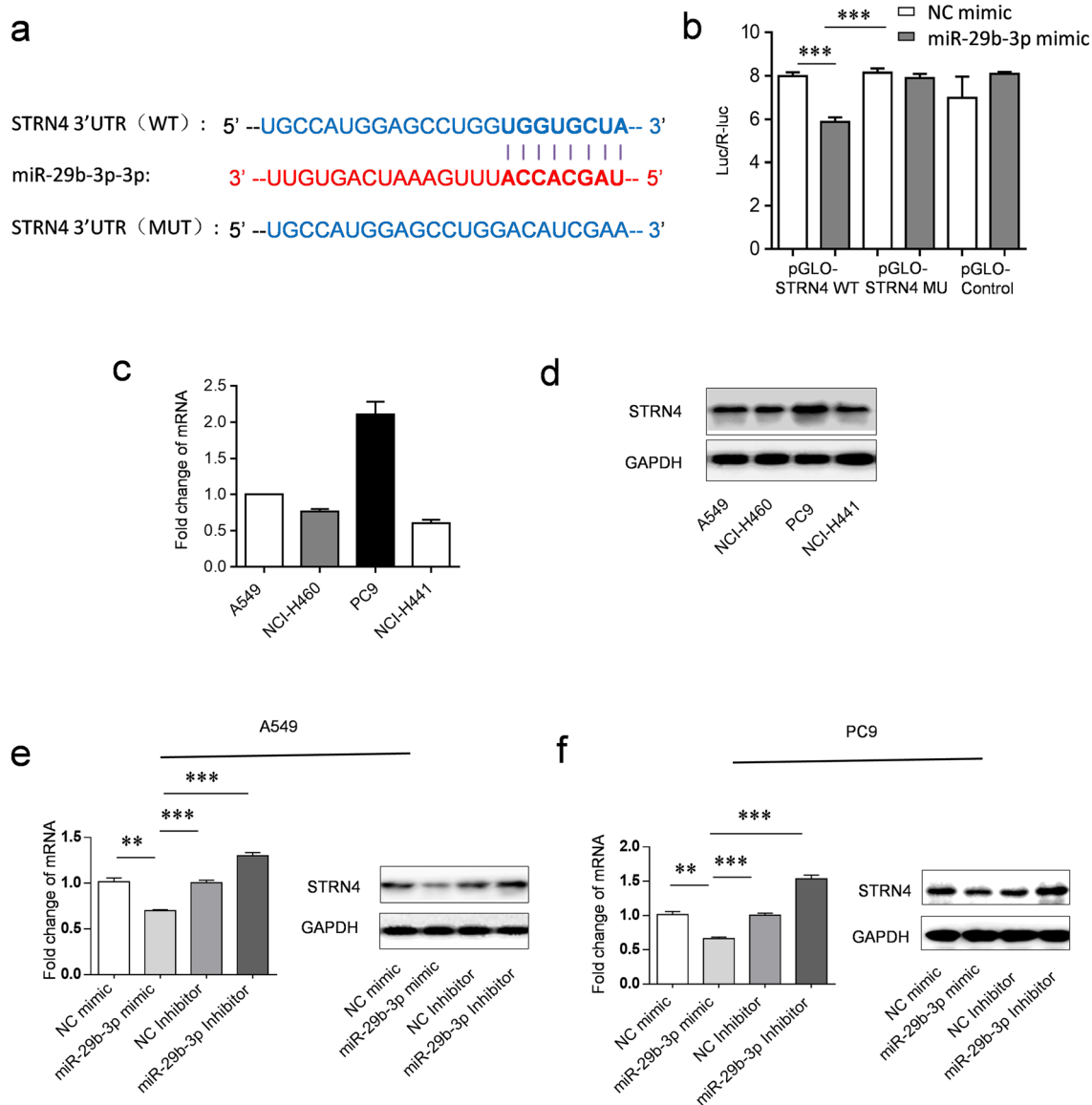
Fig. 1 miR-29b mediates STRN4 in NSCLC. **a** Luciferase reporter assays of 3′UTRs of candidate genes upon transfection of miR-29b in 293T cells. **b** Luciferase reporter assay showed that miR-29b-3p mimic reduced the intensity of fluorescence in 293T cells transfected with STRN4-WT, while it had no effect on the STRN4-MUT or control vectors. **c** qRT-PCR analysis of STRN4 mRNA expression in four tumor cell lines. **d** Representative bands showing STRN4 protein expression in four tumor cell lines by western blotting. **e** mRNA (left) and protein (right) levels of STRN4 in A549 cells transfected with mimic-control, miR-29b-3p mimic, inhibitor-control, and miR-29b-3p inhibitor. **f** mRNA (left) and protein (right) levels of STRN4 in PC9 cells transfected with mimic-control, miR-29b-3p mimic, inhibitor-control, and miR-29b-3p inhibitor. Unpaired t test for **e** and **f**. The data are represented as the mean $\pm$ SEM of three independent experiments, $**P < 0.01$, $***P < 0.001$. *WT* wild type, *MUT* mutant, *NC* negative control

expression in A549 and PC9 cells (Fig. 3a). When the STRN4 level decreased, the cell proliferation rate was significantly decreased as detected by MTT assay (Fig. 3b). We subsequently explored whether STRN4 knockdown could influence the cell cycle and apoptosis of A549 and PC9 cells. Flow cytometric analysis indicated that the knockdown of STRN4 induces G1 cell cycle arrest and a concomitant decrease in the number of cells in the S phase (Fig. 3c, d). We then stained the cells with annexin V-FITC and PI and

found that STRN4 knockdown promoted apoptosis of both cell lines mentioned above (Fig. 3e, f). To investigate the effect of STRN4 knockdown on the ability of cell migration and invasion, both A549 and PC9 were transfected with shRNA Control, shRNA STRN4-1 and shRNA STRN4-2. 24 h post-transfection, wound healing assay, and Transwell assay showed that the percentage of wound healing (Fig. 4a, b) and the migration cell per field (Fig. 4c–e) in shRNA STRN4 groups were obviously decreased compared with
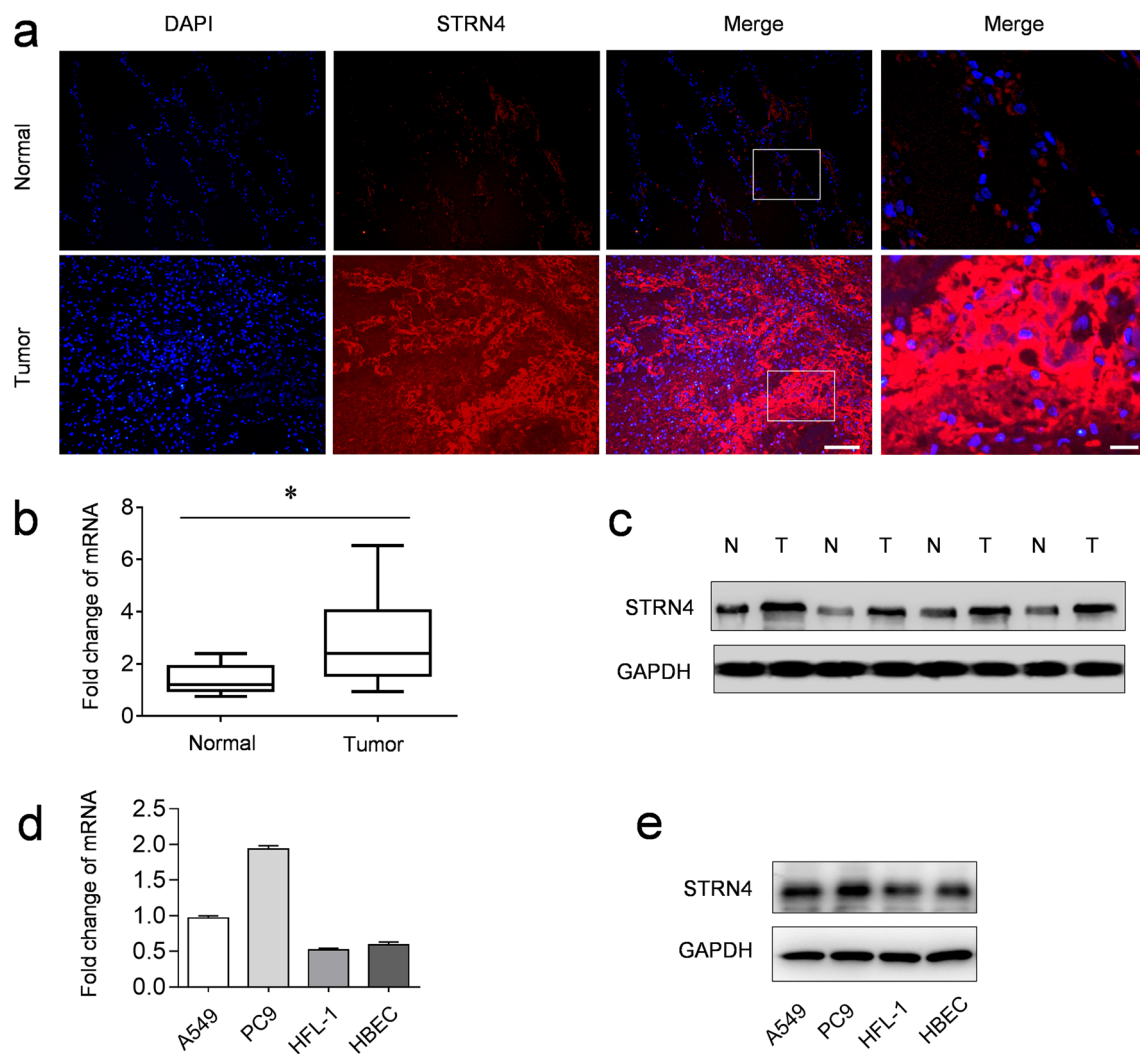
Fig. 2 Analysis of STRN4 expression in clinical samples and cell line. **a** Immunofluorescence analysis of STRN4 expression in corresponding paracancerous (normal) and NSCLC (tumor) tissue samples. Scale bar, 50 μm; panels show a close-up view of the white box, scale bar, 10 μm. **b** qRT-PCR analysis of STRN4 mRNA expression in normal and tumor tissue samples. **c** Representative bands showing STRN4 expression in normal and tumor tissues by western blotting. **d** STRN4 mRNA expression in normal and NSCLC cell lines. **e** Representative bands showing STRN4 expression in normal and NSCLC cell lines by western blotting. Unpaired t test for **b**. The data are represented as the mean $\pm$ SEM of three independent experiments, $*P < 0.05$, $***P < 0.001$. N normal tissues, T tumor tissues

the control, which indicates that the ability of A549 and PC9 cell migration and invasion was dramatically weakened by STRN4 knockdown. Together, these results suggest that STRN4 promotes the proliferation, migration, and invasion of NSCLC cells.

The miR-29b/STRN4 pathway regulates NSCLC cells proliferation, migration, invasion, and apoptosis

Since the decrease of miR-29b leads to up-regulation of STRN4 in NSCLC, this prompted us to test whether manipulation of the miR-29b/STRN4 pathway can regulate the NSCLC cells proliferation, apoptosis, migration, and invasion in vitro. We subsequently co-transfected

A549 cell with miR-29b-3p mimic and STRN4 expression plasmids. The quantative analysis showed an increased cell proliferation rate in STRN4-overexpressing groups, while a decreased cell proliferation rate in miR-29b-expressing groups by EdU staining, and miR-29b reversed the high cell proliferation rate induced by STRN4 over-expression in A549 cells (Fig. 5a). We also found higher STRN4 expression in STRN4-overexpressing groups and decreased STRN4 expression in miR-29b-expressing groups by western blotting (Fig. 5b). Flow cytometric analysis suggested that STRN4 overexpression increased A549 cell number in the S phase, while miR-29b mimic induced G1 cell-cycle arrest, and OE-STRN4 and miR-29b mimic co-transfection inhibited the S-phase cell
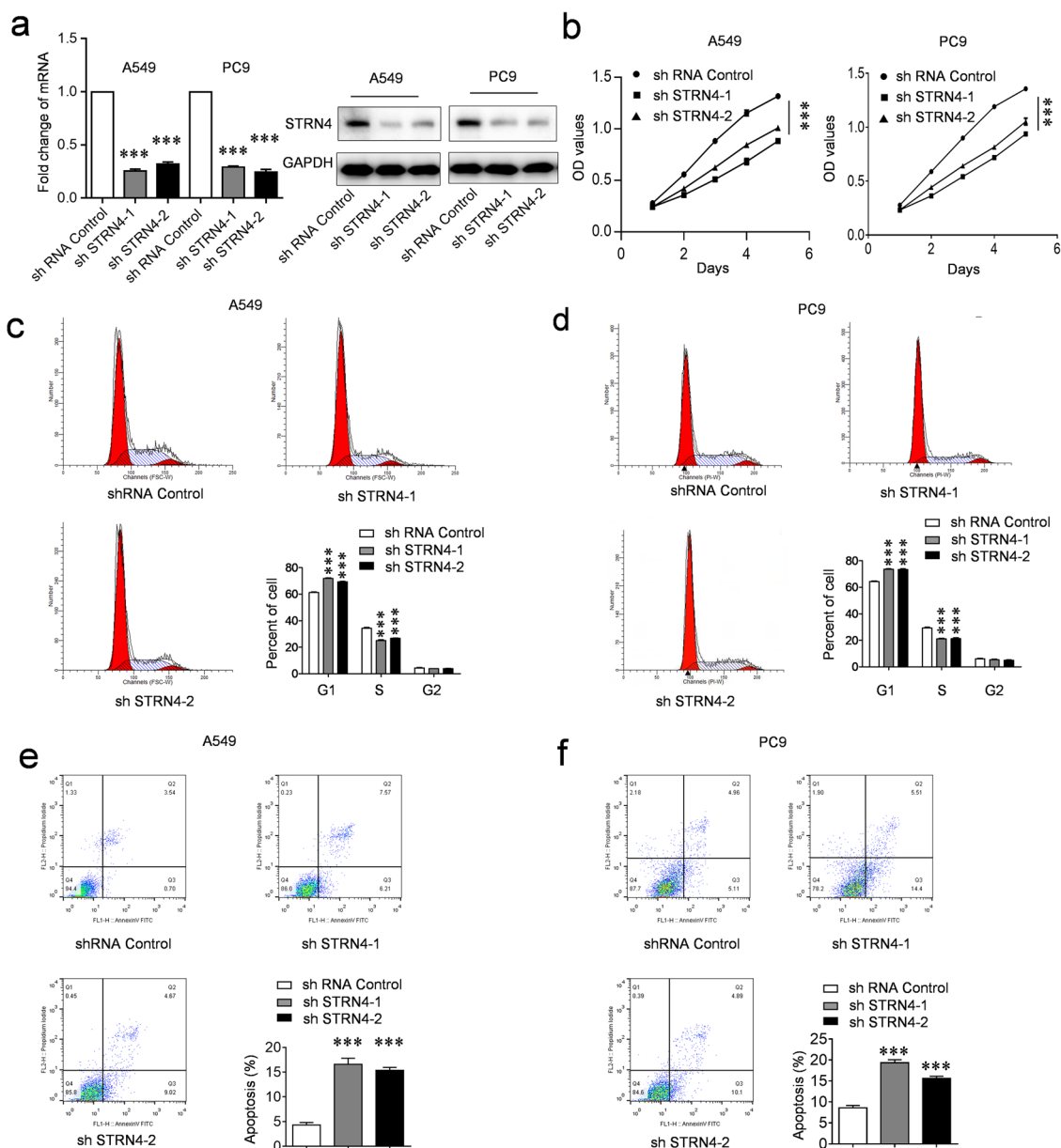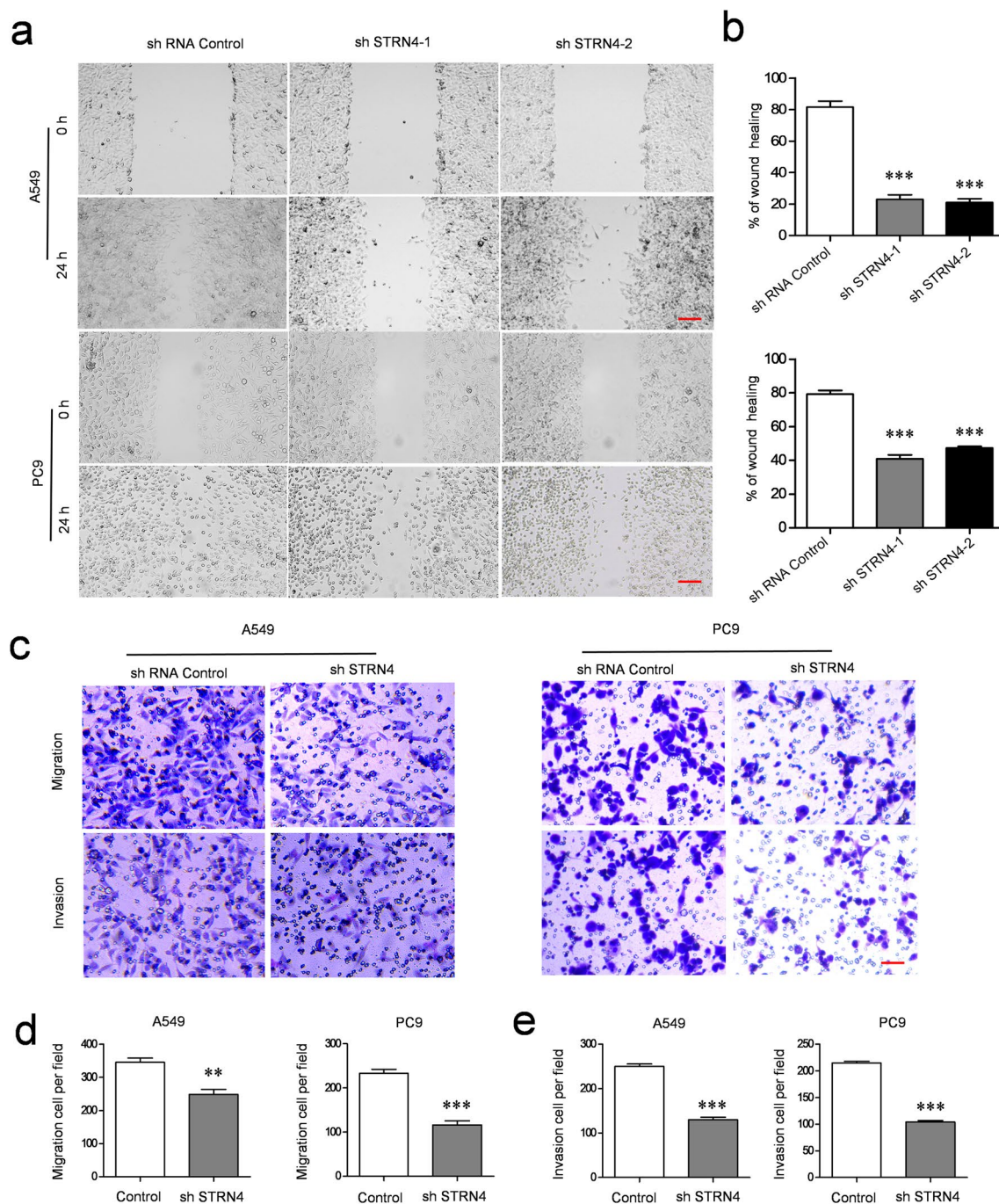
Fig. 3 Analysis of STRN4 knockdown effects on cell proliferation and apoptosis. **a** mRNA (left) and protein (right) levels of STRN4 were determined after A549 and PC9 cells were transfected with two different short hairpin RNA sequences (shRNAs) shRNA-STRN4-1 and shRNA-STRN4-2. Control shRNA served as a control. **b** Cell proliferation of A549 (left) and PC9 cells (right) was analyzed with MTT assays at indicated time points after control and STRN4 knockdown. **c, d** Cell cycle was tested and quantified by flow cytometry in A549 (**c**) and PC9 cells (**d**) transfected with shRNA-STRN4-1, shRNA-STRN4-2 or shRNA-Control. **e, f** Cell apoptosis analysis by annexin V-FITC and PI staining was tested and quantified by flow cytometry in A549 (**e**) and PC9 cells (**f**) transfected with shRNA-STRN4-1, shRNA-STRN4-2 or shRNA-Control. Unpaired t test for (**a**) and (**c**–**f**); ANOVA for **b**. The data are represented as the mean $\pm$ SEM of three independent experiments, ***$P < 0.001$. *sh* shRNA

increase induced by STRN4 overexpression (Fig. 5c, d). In addition, we also found miR-29b promoted, but STRN4 overexpression inhibited the apoptosis of A549 cells (Fig. 5e, f). Meanwhile, wound healing assay and Transwell assay showed that miR-29b was able to reverse the STRN4 overexpression-induced enhanced cell migration and invasion of A549 cells, respectively

(Fig. 5g, h). To explore the expression of tumor associated genes, proliferation genes (p21, Cyclin D1), apoptosis gene (Bax), and migration/invasion genes (MMP-9, E-cadherin) were examined in A549 cells co-transfected with different mimic/plasmid combinations mentioned above. The results showed that miR-29b promoted *p21*, *Bax*, and *E-cadherin*, but inhibited *Cyclin D1* and *MMP-9*

Fig. 4 Analysis of STRN4 knockdown effects on cell migration and invasion. **a** Representative images of the wound healing assay of indicated groups (A549-shRNA-Control cells, A549-shRNA-STRN4-1/A549-shRNA-STRN4-2 cells, PC9-shRNA-Control cells and PC9-shRNA-STRN4-1/PC9-shRNA-STRN4-2 cells). Scale bar, 50 µm. **b** Quantification of the healed wound area showed that when A549/PC9 cells were transfected with shRNA-STRN4-1/shRNA-STRN4-2, wound closure was inhibited by approximately 75% compared to shRNA-Control. **c** Images from the Transwell assay showed the invasion of indicated groups (A549-shRNA-Control cells, A549-shRNA-STRN4-1/A549-shRNA-STRN4-2 cells, PC9-shRNA-Control cells and PC9-shRNA-STRN4-1/PC9-shRNA-STRN4-2 cells). Scale bar, 50 µm. **d**, **e** Summary data of the migration and invasion of different groups (A549-shRNA-Control cells, A549-shRNA-STRN4-1/A549-shRNA-STRN4-2 cells, PC9-shRNA-Control cells and PC9-shRNA-STRN4-1/PC9-shRNA-STRN4-2 cells). Cell counts of transmigrated cells from the five photographed fields in each group. After 24 h for the migration and invasion assay, A549 and PC9 cell proliferation was decreased by STRN4 silencing. Unpaired t test for **b**, **d**, and **e**. The data are represented as the mean $\pm$ SEM of three independent experiments, $**P < 0.01$, $***P < 0.001$. *sh* shRNA
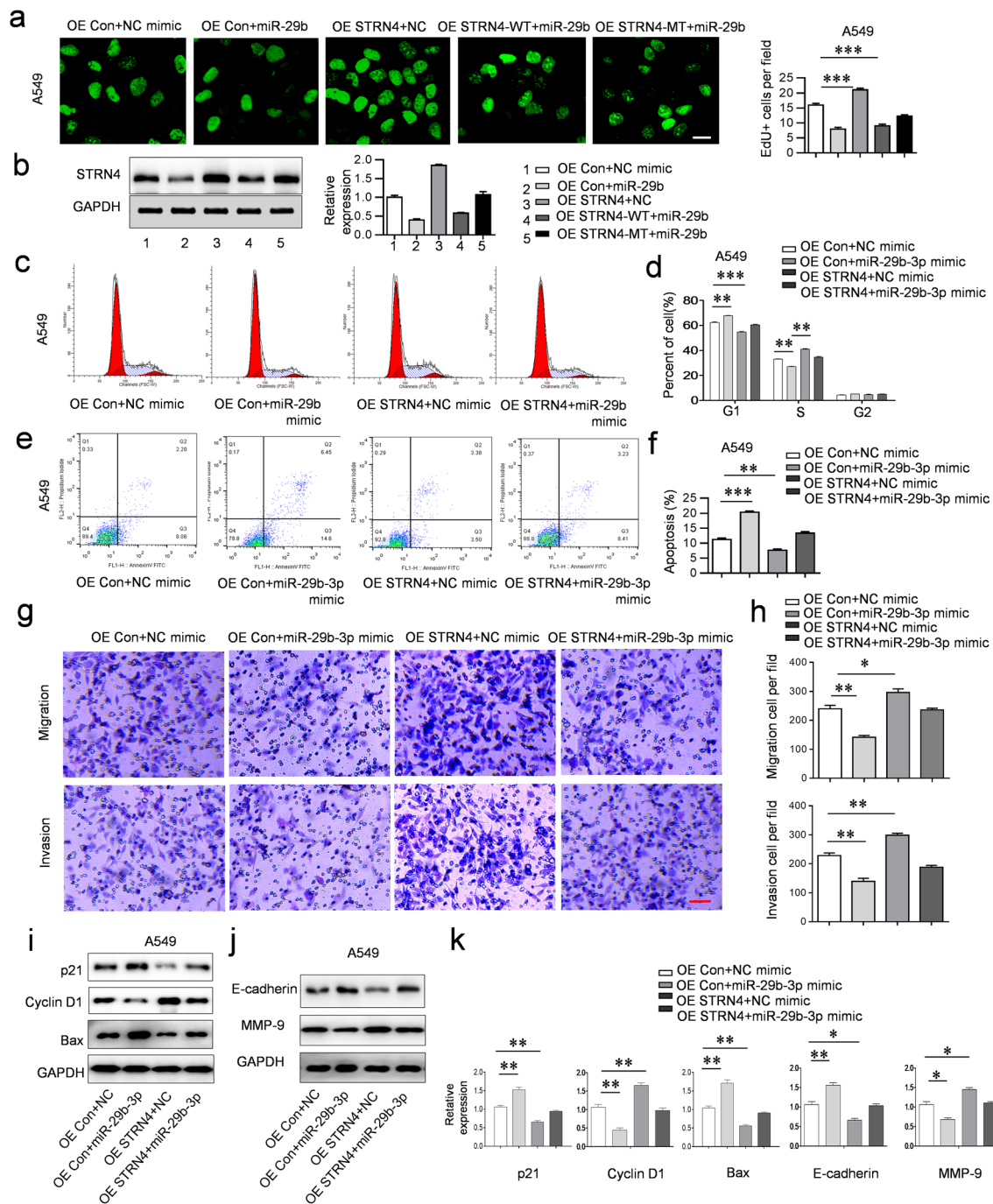
Fig. 5 miR-29b reverses STRN4-induced cell proliferation and inhibits STRN4-induced cell migration and invasion. **a** Left: images of EdU immunostaining in the A549 cells that were co-transfected with OE-control and NC-mimic, OE-control and miR-29b-3p mimic, OE-STRN4 and NC-mimic, OE-STRN4-WT and miR-29b-3p mimic or OE-STRN4-MT and miR-29b-3p mimic. Scale bar, 20 μm. Right: Bar graphs of the number of EdU⁺ cells under different conditions. **b** Expression of STRN4 protein in A549 cells transfected with OE-control and NC-mimic, OE-control and miR-29b-3p mimic, OE-STRN4 and NC-mimic, OE-STRN4-WT and miR-29b-3p mimic or OE-STRN4-MT and miR-29b-3p mimic was detected by western blotting. **c** Cell cycle was tested by flow cytometry of A549 cells under different conditions. **d** Cell cycle was quantified following flow cytometry analysis in A549 cells. **e** Cell apoptosis was measured by flow cytometry in A549 cells. **f** Cell apoptosis was quantified following flow cytometry analysis in A549 cells. **g** Representative images and **h** quantification of migration and invasion assays in A549 cells of indicated groups (OE-control and NC mimic, OE-control and miR-29b-3p mimic, OE- STRN4 and NC mimic, or OE-STRN4 and miR-29b-3p mimic). Scale bar, 50 μm. **i** Western blotting was performed to test the expression of cell proliferation and apoptosis-related genes. **j** Representative bands showing migration and invasion-related E-cadherin and MMP-9 expression. **k** Statistical data on the relative expression of tumor cell proliferation, apoptosis, migration and invasion-related genes in A549 cells under different conditions. Unpaired t test for **b**, **d**, **f**, **h**, and **k**. The data are represented as the mean ± SEM of three independent experiments, $**P < 0.01$, $***P < 0.001$. *OE* overexpression, *NC* negative control

expression, while STRN4 overexpression promoted *Cyclin D1* and *MMP-9,* but inhibited *p21, Bax*, and *E-cadherin* expression (Fig. 5i–k). In view of the critical roles played by these genes in tumor cell proliferation, apoptosis, migration, and invasion, they are potential targets of the miR-29b/STRN4 regulatory pathway in the control of NSCLC progression.

To further explore the miR-29b/STRN4 regulatory pathway in vivo, A549 cells infected by lentivirus vectors that could stably overexpress miR-29b gene or shRNA-STRN4 were subcutaneously injected into the ventral regions of six female BALB/C nude mice for 4 weeks. We observed that mice injected with NSCLC cells overexpressing miR-29b and shRNA-STRN4 formed smaller tumors compared with the control. We then measured the weight of tumors and found the weights of miR-29b overexpressing and shRNA–STRN4 tumors were significantly decreased compared with control tumors (Fig. 6a–c), and immunohistochemical staining showed that shRNA-STRN4/overexpression miR-29b was able to markedly increased the apoptosis of A549 cells (Fig. 6d).

In summary, these above results indicated that miR-29b negatively regulates the expression of STRN4 to inhibit NSCLC progression.

Discussion

Lung cancer is the most common cause of death from cancer death, and among lung cancers, NSCLC top the list of those that cause death [30]. In the present study, we found that STRN4 was highly expressed in NSCLC cell lines A549 and PC9, and miR-29b negatively modulated STRN4 expression by directly binding to the 3′-UTR region of STRN4. Excitingly, miR-29b up-regulation or STRN4 knockdown dramatically inhibited the proliferation, migration, and invasion of A549 cell both in vivo and in vitro. Thus, our research sheds light on the mechanism underlying NSCLC progression and provides new sight that will expand the clinical benefit to a broader patient population by improving outcomes in NSCLC.

The miR-29b is able to bind to specific sites typically present in the 3′-UTR of its target genes to mediate mRNA decay in lung cancer [15, 31]. Similarly, we found that miR-29b negatively regulated the expression of STRN4 both in A549 and PC9 cells, which is due to the interaction of the STRN4 3′-UTR with miR-29b. As is well known, miRNAs function through base-pairing the complementary sequences within mRNA [32], which results in silence of mRNA molecules by cleaving the mRNA strand into two pieces, destabilizing mRNA through the shortening of its poly(A) tail, or
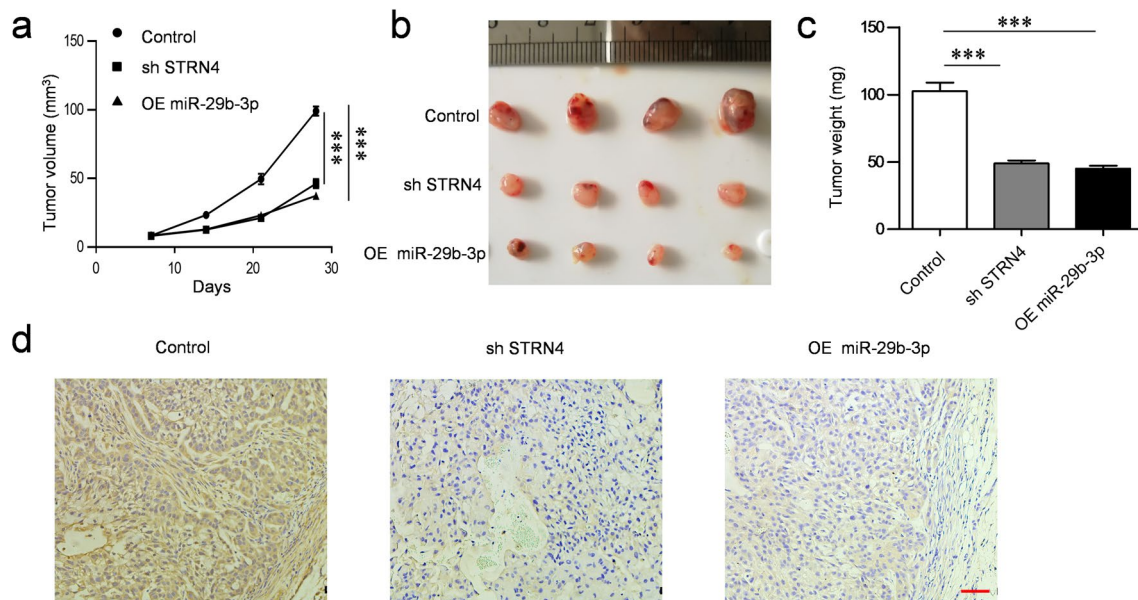
Fig. 6 Depletion of STRN4 or overexpression of miR-29b suppresses tumor growth in vivo. **a** Volume quantification of six subcutaneous tumors formed by A549-control, A549-shRNA-STRN4, and A549-miR-29b-3p mimic cells every other week after NSCLC cells injection. **b** Images of tumors removed from nude mice after 4 weeks of NSCLC cells injection. **c** Weight quantification of extracted subcutaneous tumors formed by A549-control, A549-shRNA-STRN4, and A549-miR-29b-3p mimic cells. **d** Immunohistochemical images of NSCLC tissues injected with A549-control, A549-shRNA-STRN4, and A549-miR-29b-3p mimic cell. Scale bar, 50 μm. ANOVA for **a**; unpaired *t* test for **c**. The data are represented as the mean±SEM of three independent experiments, ***$P < 0.001$. *OE* overexpression, *sh* shRNA

decreasing the translation efficiency of mRNA into proteins by ribosomes [32, 33]. In our study, we found a significant decrease of STRN4 mRNA expression both in A549 (by 31%) and PC9 (by 33%) cells after the transfection of miR-29b-3p mimic, which may result from the cleavage of the STRN4 mRNA strand by miR-29b-3p mimic. Further studies about the process that STRN4 mRNA was silenced by miR-29b are needed.

The contribution of STRN4 in many other cancers, as well as its transcriptional regulation by other molecules, has been widely investigated [6, 23, 34, 35]. However, it is still unknown whether STRN4 is associated with the progression of NSCLC. In this study, we found that STRN4 is highly expressed in NSCLC compared with the corresponding paracancerous tissues. Further experimental results showed that down-regulation of STRN4 inhibited the proliferation, migration, and invasion of NSCLC cells. How does the STRN4 expression affect NSCLC? Our study showed that the STRN4 overexpression promoted the proliferation, invasion, and survival of A549 cells probably by increasing the level of Cyclin D1 and MMP-9, and by decreasing the level of p21, Bax, and E-cadherin. In fact, p21, Cyclin D1, and Bax play important roles in the regulation of NSCLC cell cycle [14], proliferation [36, 37], and apoptosis [38, 39]. Timosaponin AIII can inhibit migration and invasion of human NSCLC A549 cells via attenuations of MMP-2 and MMP-9 by inhibitions of ERK1/2, Src/FAK and β-catenin signaling pathways [40]. Loss of E-cadherin activates EGFR–MEK/ERK signaling that promotes NSCLC cells invasion via the ZEB1/MMP2 axis [41]. Therefore, our results indicate that miR-29b/STRN4 pathway modulated the progression of NSCLC probably by regulating the expression of p21, Cyclin D1, Bax, MMP-9, and E-cadherin. We advocate for further studies to elucidate how these downstream targets are regulated by STRN4 in NSCLC progression.

In conclusion, our research defines a new miR-29b/STRN4 inhibitory pathway, dysfunction of which may account for the progression of NSCLC. The STRN4 was highly expressed in NSCLC, and inhibition of STRN4 leads to aberrant expression of tumor associated genes. This opens a new window for therapeutic intervention in NSCLC.

Compliance with ethical standards

Conflict of interest The authors declare no potential conflicts of interest.

Ethical approval Written informed consent was obtained from all the participants. The protocols for human specimen studies were approved by the Ethics Committee of the West China Second University Hospital of Sichuan University, and were conducted in agreement with the principles set forth in the Declaration of Helsinki. All animal protocols were approved by the Animal Care and Use Committee of the West China Second University Hospital of Sichuan University.

References

1. Torre LA, et al. Global cancer statistics, 2012. CA Cancer J Clin. 2015;65(2):87–108.
2. Herbst RS, et al. The biology and management of non-small cell lung cancer. Nature. 2018;553(7689):446–54.
3. Ambros V. MicroRNA pathways in flies and worms: growth, death, fat, stress, and timing. Cell. 2003;113(6):673–6.
4. Volinia S, et al. A microRNA expression signature of human solid tumors defines cancer gene targets. Proc Natl Acad Sci. 2006;103(7):2257–61.
5. Jiang H, et al. Diverse roles of miR-29 in cancer. Oncol Rep. 2014;31(4):1509–16.
6. Wang Y, et al. The role of miRNA-29 family in cancer. Eur J Cell Biol. 2013;92(3):123–8.
7. Suda K, et al. Biological and clinical significance of KRAS mutations in lung cancer: an oncogenic driver that contrasts with EGFR mutation. Cancer Metastasis Rev. 2010;29(1):49–60.
8. Thakur S, Brenner C. KRAS-driven miR-29b expression is required for tumor suppressor gene silencing. Oncotarget. 2017;8(43):74755–66.
9. Ling Q, et al. Special suppressive role of miR-29b in HER2-positive breast cancer cells by targeting Stat3. Am J Transl Res. 2015;7(5):878–90.
10. Zhang L, et al. The relationship between microRNAs and the STAT3-related signaling pathway in cancer. Tumor Biol. 2017;39(7):1–11.
11. Li Y, et al. Chemotherapy-mediated miR-29b expression inhibits the invasion and angiogenesis of cervical cancer. Oncotarget. 2017;8(9):14655–65.
12. Wang H, et al. MicroRNA-29b attenuates non-small cell lung cancer metastasis by targeting matrix metalloproteinase 2 and PTEN. J Exp Clin cancer Res. 2015;34(59):1–12.
13. Chen B, et al. A regulatory circuitry comprising TP53, miR-29 family, and SETDB1 in non-small cell lung cancer. Biosci Rep. 2018;38(5):1–10.
14. Tang Y, et al. Radiation-induced miR-208a increases the proliferation and radioresistance by targeting p21 in human lung cancer cells. J Exp Clin cancer Res. 2016;35(7):1–14.
15. Mizuno K, et al. Tumor-suppressive microRNA-29 family inhibits cancer cell migration and invasion directly targeting LOXL2 in lung squamous cell carcinoma. Int J Oncol. 2016;48(2):450–60.
16. Bartoli M, et al. Interaction of calmodulin with striatin, a WD-repeat protein present in neuronal dendritic spines. J Biol Chem. 1998;273(35):22248–53.
17. Gaillard S, et al. Targeting of proteins of the striatin family to dendritic spines: role of the coiled-coil domain. Traffic. 2006;7(1):74–84.
18. Gaillard S, et al. Striatin, a calmodulin-dependent scaffolding protein, directly binds caveolin-1. FEBS Lett. 2001;508(1):49–52.

19. Castets F, et al. Zinedin, SG2NA, and striatin are calmodulin-binding, WD repeat proteins principally expressed in the brain. J Biol Chem. 2000;275(26):19970–7.
20. Bartoli M, et al. Down-regulation of striatin, a neuronal calmodulin-binding protein, impairs rat locomotor activity. J Neurobiol. 1999;40(2):234–43.
21. Kachidian P, et al. Relationships between striatin-containing neurons and cortical or thalamic afferent fibres in the rat striatum. An ultrastructural study by dual labelling. Neuroscience. 1998;85(1):111–22.
22. Salin P, et al. Distribution of Striatin, a newly identified calmodulin-binding protein in the rat brain: an in situ hybridization and immunocytochemical study. J Comp Neurol. 1998;397(1):41–59.
23. Wong M, et al. Silencing of STRN 4 suppresses the malignant characteristics of cancer cells. Cancer Sci. 2014;105(12):1526–32.
24. Collins CS, et al. A small interfering RNA screen for modulators of tumor cell motility identifies MAP4K4 as a promigratory kinase. Proc Natl Acad Sci. 2006;103(10):3775–80.
25. Hyodo T, et al. Misshapen-like kinase 1 (MINK1) is a novel component of striatin-interacting phosphatase and kinase (STRIPAK) and is required for the completion of cytokinesis. J Biol Chem. 2012;287(30):25019–29.
26. Shitashige M, et al. Traf2-and Nck-interacting kinase is essential for Wnt signaling and colorectal cancer growth. Cancer Res. 2010;70(12):5024–33.
27. Fan C, et al. MicroRNA-873 inhibits colorectal cancer metastasis by targeting ELK1 and STRN4. Oncotarget. 2019;10(41):4192–204.
28. Sartini D, et al. Pokemon proto-oncogene in oral cancer: potential role in the early phase of tumorigenesis. Oral Dis. 2015;21(4):462–9.
29. Rheinbay E, et al. Recurrent and functional regulatory mutations in breast cancer. Nature. 2017;547(7661):55–60.
30. Molina JR et al., Non-small cell lung cancer epidemiology, risk factors, treatment, and survivorship, Mayo Clinic Proceedings. Amsterdam: Elsevier; 2008, pp. 584–594.
31. Fabbri M, et al. MicroRNA-29 family reverts aberrant methylation in lung cancer by targeting DNA methyltransferases 3A and 3B. Proc Natl Acad Sci. 2007;104(40):15805–10.
32. Bartel DP. MicroRNAs: target recognition and regulatory functions. Cell. 2009;136(2):215–33.
33. Fabian MR, et al. Regulation of mRNA translation and stability by microRNAs. Annu Rev Biochem. 2010;79:351–79.
34. Jiang F, et al. Pro-oncogene pokemon promotes prostate cancer progression by inducing STRN4 expression. J Cancer. 2019;10(8):1833–45.
35. Madsen CD, et al. STRIPAK components determine mode of cancer cell migration and metastasis. Nat Cell Biol. 2015;17(1):68–80.
36. Gautschi O, et al. Cyclin D1 in non-small cell lung cancer: a key driver of malignant transformation. Lung Cancer. 2007;55(1):1–14.
37. Li Y, et al. Curcumin inhibits human non-small cell lung cancer A549 cell proliferation through regulation of Bcl-2/Bax and cytochrome C. Asian Pac J Cancer Prev. 2013;14(8):4599–602.
38. Jiang H, et al. Paris saponin I induces apoptosis via increasing the Bax/Bcl-2 ratio and caspase-3 expression in gefitinib-resistant non-small cell lung cancer in vitro and in vivo. Mol Med Rep. 2014;9(6):2265–72.
39. Chakraborty S, et al. Restoration of p53/miR-34a regulatory axis decreases survival advantage and ensures Bax-dependent apoptosis of non-small cell lung carcinoma cells. FEBS Lett. 2014;588(4):549–59.
40. Jung O, et al. Timosaponin AIII inhibits migration and invasion of A549 human non-small-cell lung cancer cells via attenuations of MMP-2 and MMP-9 by inhibitions of ERK1/2, Src/FAK and β-catenin signaling pathways. Bioorg Med Chem Lett. 2016;26(16):3963–7.
41. Bae G-Y, et al. Loss of E-cadherin activates EGFR-MEK/ERK signaling, which promotes invasion via the ZEB1/MMP2 axis in non-small cell lung cancer. Oncotarget. 2013;4(12):2512–22.